




8-2015

Cellular localization and metabolomic analysis of the *Arabidopsis thaliana* Major Intrinsic Protein NIP2;1: A root-specific lactic acid transporter induced in response to hypoxic stress

Taylor K. Fuller

University of Tennessee - Knoxville, tfuller4@vols.utk.edu

Follow this and additional works at: https://trace.tennessee.edu/utk_chanhonoproj

 Part of the [Biochemistry Commons](#), [Molecular Biology Commons](#), and the [Plant Sciences Commons](#)

Recommended Citation

Fuller, Taylor K., "Cellular localization and metabolomic analysis of the *Arabidopsis thaliana* Major Intrinsic Protein NIP2;1: A root-specific lactic acid transporter induced in response to hypoxic stress" (2015). *University of Tennessee Honors Thesis Projects*.
https://trace.tennessee.edu/utk_chanhonoproj/1856

This Dissertation/Thesis is brought to you for free and open access by the University of Tennessee Honors Program at Trace: Tennessee Research and Creative Exchange. It has been accepted for inclusion in University of Tennessee Honors Thesis Projects by an authorized administrator of Trace: Tennessee Research and Creative Exchange. For more information, please contact trace@utk.edu.

Cellular localization and metabolomic analysis of the *Arabidopsis thaliana* Major Intrinsic
Protein NIP2;1: A root-specific lactic acid transporter induced in response to hypoxic
stress

Chancellor's Honors Program
Department of Biochemistry, Cellular and Molecular Biology
University of Tennessee, Knoxville

Taylor K. Fuller

May 2015

Daniel M. Roberts

Ansul Lokdarshi

ACKNOWLEDGEMENTS

I would sincerely like to thank Dr. Dan Roberts, my research mentor, for providing me with the opportunity to work in his laboratory, for his enduring patience and encouragement, and for proving to me just how interesting plants can be. I would also like to thank Ansul Lokdarshi for his countless hours of guidance, for patiently helping me discover my inner scientist, and for always believing in me. Finally, I would like to thank the other members of the Roberts Lab for helping me along the way, along with the Chancellor's Honors Program and Department of Biochemistry, Cellular and Molecular Biology for their gracious support.

ABSTRACT

Plants depend upon a constant supply of molecular oxygen from their environment to support energy production via respiration and other life-sustaining processes. Oxygen deprivation resulting from flooding, water logging, or even poor aeration of the soil becomes a primary cause of plant stress. Oxygen deficit leads to severe depression of respiration resulting in deficiency in life-supporting adenylate charge, accumulation of toxic metabolites and cytosolic acidification. Central to the responses toward anaerobiosis is the induction of a special class of genes termed as the anaerobic response polypeptides (ANPs) that include glycolytic and fermentation enzymes, various signal transduction proteins involved in coordinating adaptation/survival responses toward anaerobiosis. Here, we have characterized the cellular localization

and metabolic function of the *Arabidopsis thaliana* core anaerobic response gene *AtNIP2;1* during flooding stress conditions. *AtNIP2;1* is a member of the Nodulin 26 intrinsic proteins (NIPs), which are plant-specific, highly conserved water and solute transport proteins with structural and functional homology to soybean nodulin 26. Protein blot analysis of the *NIP2;1 promoter::NIP2;1:YFP* (yellow fluorescent protein) seedlings challenged with hypoxia results in the accumulation of NIP2;1-YFP in a time-dependent manner exclusively in the roots. Confocal fluorescence microscopy scans of the hypoxic roots show the protein localized on the plasma membrane within the central stele area and likely the phloem vascular tissue, through which NIP2;1 could act to transport lactic acid. Furthermore, functional analysis of the NIP2;1 protein by global metabolomics profile of the 6 hr hypoxia challenged T-DNA knockout seedlings versus wild type shows that lactic acid levels were elevated in knockout plants, suggesting that removal of NIP2;1 results in lactic acid accumulation. This supports the previous *in vitro* studies showing NIP2;1 as a lactic acid channel protein.

The classical metabolic response of plant roots to anaerobic stress is the rapid and transient induction of lactic acid fermentation followed by a switch to sustained ethanolic fermentation to prevent cytosolic acidity (the Davies-Roberts hypothesis). One hypothetical role of NIP2;1 is to mediate lactic acid efflux to prevent cytosolic acidosis by selectively localizing to phloem cells of the stele, which contributes to the overall adaptive response of the plant towards anaerobic stress.

TABLE OF CONTENTS

<u>CHAPTER</u>		<u>PAGE</u>
I.	INTRODUCTION	5
1.1	Anaerobic metabolism and waterlogging	5
1.2	Structures and functions of major intrinsic protein aquaporins	8
1.3	The NIP subfamily of plant MIPs	10
1.4	AtNIP2;1 structure, functions and localization	11
II.	MATERIALS AND METHODS	13
2.1	Plant growth conditions and stress treatment	13
2.2	Experimental approach	14
	a. Generation of NIP2;1promoter::NIP2;1:YFP (recombineering) plants	14
	b. Immunochemical techniques	15
	c. Genotyping of NIP2;1promoter::NIP2;1:YFP seedlings	16
2.3	Microscopy	17
2.4	Metabolomics	17

a.	Sample preparation	18
b.	UPLC-HRMS metabolomics analysis	19
III.	RESULTS	21
3.1	NIP2;1 levels in shoot and root tissue during hypoxia	21
3.2	NIP2;1 subcellular localization	22
3.3	Metabolic profile of WT and AtNIP2;1 T-DNA knockout	24
IV.	DISCUSSION AND CONCLUSION	27
4.1	NIP2;1 is a lactic acid transporter induced by hypoxic stress exclusively in roots	29
4.2	NIP2;1 is localized to the phloem of the root stele	31
V.	REFERENCES	33

I. INTRODUCTION

1.1 Anaerobic metabolism and waterlogging

Similar to all aerobic organisms, higher plants rely on a source of molecular oxygen from their environment to undergo aerobic respiration critical for energy production, and also utilize oxygen as a substrate for many other vital oxidations and oxygenation reactions. As a result, plants are equipped with biochemical and morphological features necessary for facilitating the distribution of oxygen to cells (Vartapetian & Jackson, 1997). Because of this strictly aerobic lifestyle, environmental conditions that lead to hypoxic or anoxic conditions represent a severe stress. For example, most plants are highly sensitive to waterlogging, which results in an insufficient supply to oxygen to submerged tissues, since diffusion of oxygen through water is much slower than through air (Jackson & Colmer, 2005).

When there is a deficit of available oxygen, which would normally serve as the final electron acceptor in aerobic respiration, plants undergo a metabolic switch to anaerobic fermentation in an attempt to sustain basal energy production through glycolysis (Buchanan, Gruissem, & Jones, 2000). During fermentation, following the breakdown of glucose into pyruvate, pyruvate then can ultimately either be converted into lactic acid or ethanol and carbon dioxide in order to regenerate NAD^+ to continue ATP production within glycolysis (Fig. 1). The two types of anaerobic fermentation are ethanolic fermentation and lactic acid fermentation. Under ethanolic fermentation, pyruvate, the

product of glycolysis, is converted to acetaldehyde and carbon dioxide via the enzyme pyruvate decarboxylase. Acetaldehyde is then converted to ethanol via the alcohol dehydrogenase enzyme. On the other hand, lactic acid fermentation results in the conversion of pyruvate from glycolysis into lactic acid via the enzyme lactate dehydrogenase. This metabolic switch leads to a reduction in energy due to a lower ATP output but is essential to sustain glycolysis. Besides the lower energy production, the accumulation of fermentation products ethanol, lactic acid, and particularly acetaldehyde, which are toxic metabolites, damages the cell due to acidosis or increased reactivity (Buchanan et al., 2000).

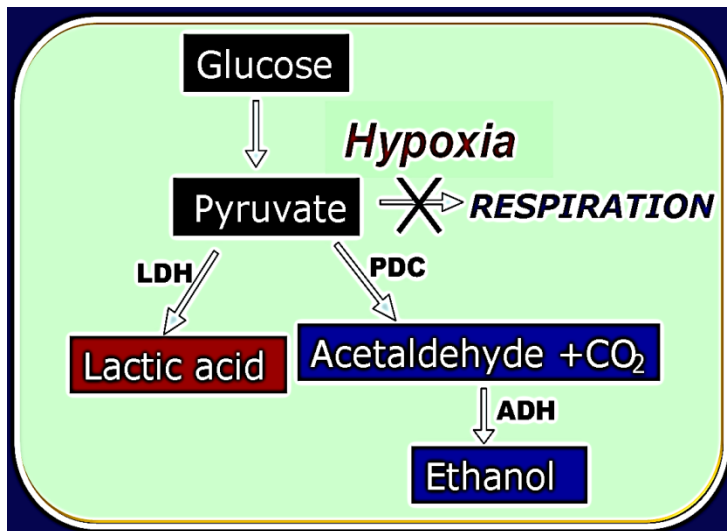


Figure 1. Fermentation metabolism in plants. Glucose is converted to pyruvate during glycolysis, but in the absence of oxygen is not able to undergo further catabolism by respiration. Instead, pyruvate is further processed by lactic acid or ethanolic fermentation to recycle NAD^+ to glycolysis. LDH, lactate dehydrogenase; PDC, pyruvate

decarboxylase; ADH, alcohol dehydrogenase.

Plants have both biochemical and developmental adaptations to compensate for flooding stress. Various phenotypes can develop to aid in circumventing this stress, including upward bending of leaves, increased shoot elongation, development of interwoven air-filled voids known as aerenchyma, generation of barriers to radial oxygen

loss in root tissue, development of new root surfaces, creation of gas films on surfaces of leaves, and changes in general leaf structure and pressurized gas flow (Voeselek & Bailey-Serres, 2015). Additionally, changes in ATP production, modified protein synthesis and metabolite transport, and increased mRNA transcription associated with anaerobic response are also observed (Voeselek & Bailey-Serres, 2015). The onset of anaerobic metabolism results in the increased transcription of genes and production of enzymes active in fermentation, including lactate dehydrogenase, pyruvate decarboxylase, and alcohol dehydrogenase (Fig. 2 & 3). Additionally, increased levels of the mRNA transcripts of these relevant genes are more pronounced in the roots (Bailey-Serres & Colmer, 2014). These responses allow the plant to sustain energy metabolism. Also included in this stress response are the induction of other core hypoxia-induced genes, identified by transcriptomics following hypoxia treatment (Mustroph et al., 2009). Among these core hypoxia-induced genes is the membrane channel protein AtNIP2;1, a transporter of lactic acid, which is the subject of the present work.

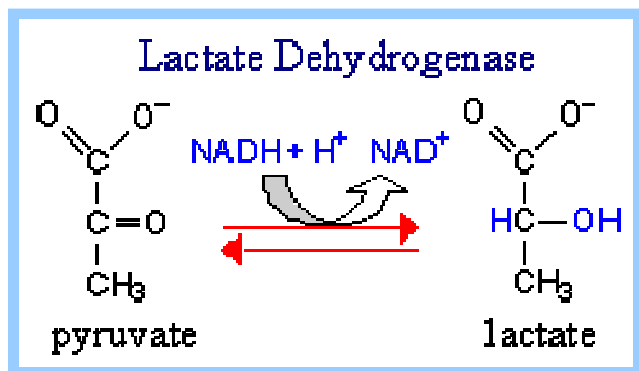


Figure 2. Lactic acid fermentation. Pyruvate produced by glycolysis is converted to lactate via the enzyme lactate dehydrogenase.

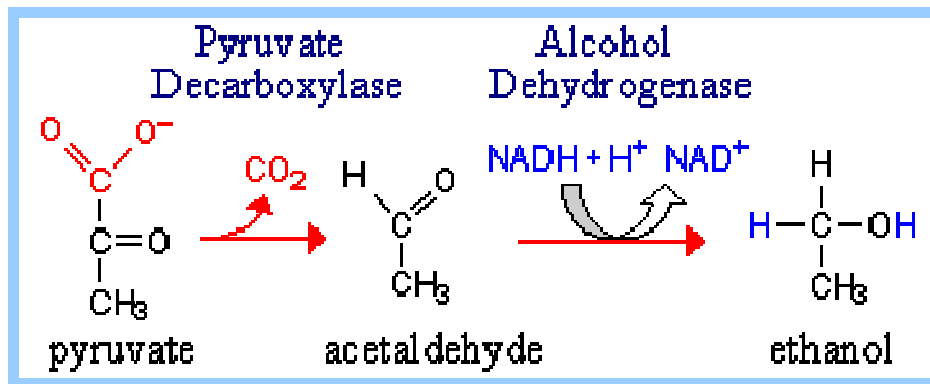


Figure 3. Ethanolic fermentation.

Pyruvate produced by glycolysis is converted to acetaldehyde and carbon dioxide via the enzyme pyruvate

decarboxylase and then to ethanol via the enzyme alcohol dehydrogenase.

1.2 Structures and functions of major intrinsic protein aquaporins

Major intrinsic proteins (MIPs) are an abundant family of integral membrane channel proteins, which includes the aquaporin superfamily, that transports water and uncharged solutes (Gomes et al., 2009). The first discovered MIP was the major bovine lens fiber cell membrane protein, initially believed to serve as a gap junction channel (Gorin, Yancey, Cline, Revel, & Horwitz, 1984). However, seminal work in 1992 by Nobel Prize winning scientist Peter Agre showed that MIPs are protein water channels that facilitate the rapid movement of water in response to osmotic gradients (Preston, Carroll, Guggino, & Agre, 1992; Smith & Agre, 1991). MIPs are found in all kingdoms of life including plants, animal and microbial species. For instance, thirteen unique aquaporin proteins have been identified in humans (Sorani, Manley, & Giacomini, 2008). Their physiological significance is obvious after noting that genetic aquaporin defects result in abnormal water homeostasis that result in various types of diseases, including diabetes insipidus and cataracts (Sorani et al., 2008).

MIPs form homotetramers with each subunit assuming a conserved hourglass fold structure, consisting of six transmembrane helices and five loops of hydrophilic amino and carboxyl termini. Additionally, two of these loop regions are composed of hydrophobic asparagine-proline-alanine (NPA) sequences, half helices that fold back into the protein and form a portion of the aquaporin pore (Fig. 4). This structure allows for the formation of an hourglass with a contracted pore in the middle of the membrane bilayer (Jung, Preston, Smith, Guggino, & Agre, 1994).

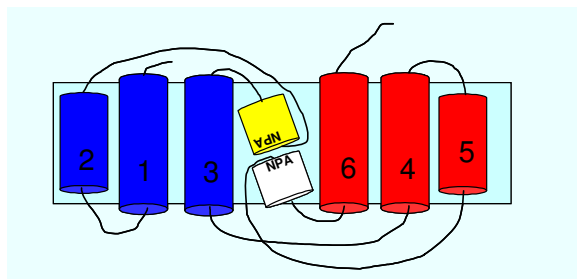
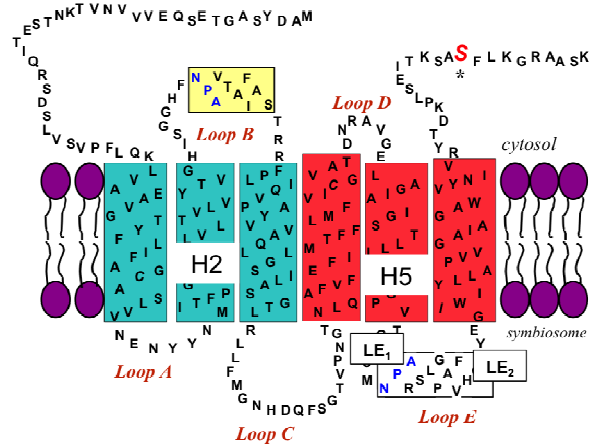


Figure 4. Membrane topology of the MIP superfamily.

Highly conserved NPA motifs are shown in yellow and white (loops B and

E). Selective ar/R filter residues are seen in helix 2 (H2), helix 5 (H5), and loop E (LE₁ and LE₂, respectively). Models are from (Wallace & Roberts, 2004).



The substrate selectivity of MIPs differs depending on the composition of the aromatic/arginine (ar/R) selectivity filter. This region is formed by four amino acids that converge and form the most constricted area of the pore (Fig. 4). In addition, two conserved NPA motifs containing asparagine in the middle of the pore consist of amide groups that also interact with transported water or glycerol molecules (Fu et al., 2000; Sui, Han, Lee, Walian, & Jap, 2001).

1.3 The NIP subfamily of plant MIPs

During higher plant evolution, the MIP family expanded with over 30 genes encoding proteins found in all plant genomes. These proteins are divided into four phylogenetic families, including plasma membrane intrinsic proteins (PIPs), tonoplast intrinsic proteins (TIPs), nodulin 26-like intrinsic proteins (NIPs), and small and basic intrinsic proteins (SIPs) (Chaumont, Moshelion, & Daniels, 2005; Johansson, Karlsson, Johanson, Larsson, & Kjellbom, 2000; Maurel, Verdoucq, Luu, & Santoni, 2008). This diversification of plant MIP genes was also accompanied by a diversification of the structure of the pore and transport functions (Ludewig & Dynowski, 2009; Wallace & Roberts, 2004). For example, while animal aquaporins/MIPs have two types of ar/R filters, *Arabidopsis* MIPs have eight types, reflecting additional transport functions for these proteins (Wallace & Roberts, 2004).

Nodulin 26-like intrinsic proteins (NIPs) are highly conserved water and solute transport proteins that are only found in plants, and which are structurally and functionally similar to soybean nodulin 26, the first member of the family discovered (Wallace, Choi, & Roberts, 2006). *Arabidopsis thaliana* contains nine NIP genes (Johanson et al., 2001). These are further categorized into two subgroups (Fig. 5); NIP subgroup I proteins are more similar to soybean nodulin 26 with aquaglyceroporin activities, while NIP subgroup II proteins exhibit low water permeability and transport solutes such as urea and boron (Choi & Roberts, 2007; Tanaka, Wallace, Takano, Roberts, & Fujiwara, 2008; Wallace et al., 2006; Wallace & Roberts, 2004).

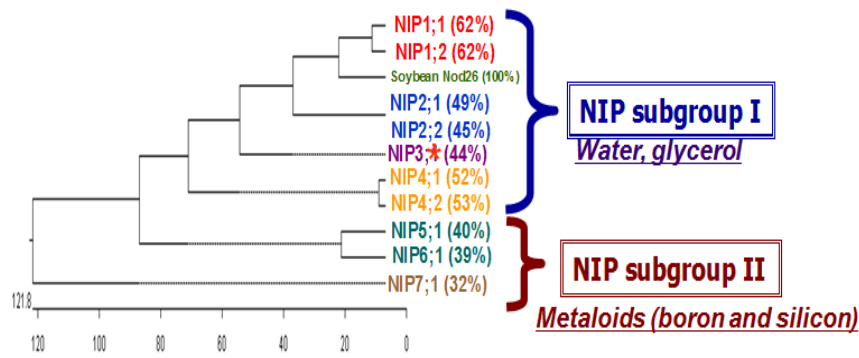


Figure 5. Phylogenetic tree of Nodulin 26-Like Intrinsic Proteins from Arabidopsis.

A phylogenetic tree was constructed using the protein sequences of the indicated Arabidopsis NIP proteins

(Johanson et al., 2001) and soybean nodulin 26. The % shown indicates the level of amino acid sequence identity to nodulin 26. The two pore families (NIP I and NIP II) based on (Wallace & Roberts, 2004) are indicated. *AtNIP2;1* belongs to the NIP subgroup I protein family. The scale below the phylogenetic tree indicates the relative number of amino acid substitutions.

1.4 *AtNIP2;1* structure, functions and localization

Arabidopsis *NIP2;1* (*AtNIP2;1*) is a member of the NIP subgroup I protein family, is root specific, and is among the core hypoxia induced genes in *Arabidopsis thaliana*.

AtNIP2;1 is expressed at a basal level in root tips and the stele of mature root tissues, but then is greatly upregulated following water logging and hypoxic stress (Choi & Roberts, 2007). Unlike other NIP subgroup I proteins, work by Choi and Roberts (2007) shows that *NIP2;1* has very unusual selectivity. Instead of water or glycerol, *NIP2;1* showed specific transport of protonated lactic acid. Since this is a toxic fermentation product, it can be argued that the function of *AtNIP2;1* is to transport lactic acid out of cells to minimize negative physiological effects (cytosolic acidosis) resulting from lactic acid accumulation.

The findings that *AtNIP2;1* encodes a lactic acid transport protein that is induced by anaerobic conditions suggests that *AtNIP2;1* functions as an adaptive measure to respond to lactic acid fermentation under anaerobic stress (Choi & Roberts, 2007). However, the specific location of this transporter in root cells and the effects of a gene knockout on hypoxia metabolism have yet to be studied. The purpose of the present study is twofold: 1. The use of fluorescent protein fusions of *AtNIP2;1* protein to perform cellular localization analyses in hypoxic *Arabidopsis* roots; and 2. To assess the effects of a gene knockout of *AtNIP2;1* in *Arabidopsis thaliana* on the global metabolic profile with major focus on lactic acid.

II. MATERIALS AND METHODS

2.1 Plant growth conditions and stress treatment

Arabidopsis thaliana ecotype Columbia 0 seeds were surface sterilized with 50% (v/v) ethanol for 1 minute, and then with 50% (v/v) sodium hypochlorite (bleach) containing 0.1% (v/v) Tween 20 for 15 minutes. The seeds were rinsed five times with sterile distilled water and were planted on 1X Murashige and Skoog (MS) agar medium with 3% (w/v) sucrose (Cat # M9274; Sigma-Aldrich, St. Louis, MO). The seeds were stratified at 4° C for 2 days, and were then transferred to a growth chamber and were grown under cool white fluorescent lights (76-100 $\mu\text{mol m}^{-2} \text{s}^{-1}$) with a long day (LD) cycle of 16 hr light/8 hr dark at 22° C.

For hypoxia treatments, 12 day-old *Arabidopsis* seedlings grown vertically on MS agar medium were completely submerged in water purged with a continuous supply of nitrogen gas. Treatment was performed in the dark and the time of hypoxia was initiated at $\leq 2\%$ dissolve O_2 monitored with an oxygen monitor (YSI model 55). For control treatments, seedlings were air treated in same dark conditions. At the end of treatments, shoot and root tissues were separated and flash frozen in liquid N_2 for protein blot analysis. Post-treatment whole seedlings were used for imaging analysis.

2.2 Experimental approach

a. Generation of *NIP2;1promoter::NIP2;1:YFP* (recombineering) plants

Recombineering lines containing *NIP2;1* fused to three copies of YFP at the C-terminus (*NIP2;1-YFP*) were generated as described in (Zhou, Benavente, Stepanova, & Alonso, 2011). The JAtY clone information and primers for *NIP2;1* (JAtY57L18) were obtained from Arabidopsis Tagging (<http://arabidopsislocalizome.org>). JAtY57L18 was purchased from the Genome Analysis Center (Norwich, UK). The *E. coli* recombineering strain SW105 was purchased from Frederick National Laboratory for Cancer Research and the recombineering cassette with 3X Ypet was generously provided by Dr. Jose Alonso (North Carolina State University). The cassette was introduced to the C-terminus of *NIP2;1* by PCR using Rec_F and R primers (Table 1). The 3X Ypet tagged JAtY57L18 clone was transformed into *Agrobacterium tumefaciens* GV3101 and transgenic recombineering strains were selected by the procedure of (Zhou et al., 2011) using the 3xYFP_SEQ primers listed in Table 1. Growth of recombineering transgenic plants was done by selection on 1X MS media supplemented with 25 µg/ml Basta (Chem Service-N12111; the recombineering seedling lines were provided by Dr. Tian Li, a former graduate student in the Roberts Lab).

Table 1. Sequences of primers used for generation of *NIP2;1promoter::NIP2;1:YFP* (recombineering) plants.

NAME	SEQUENCE (5' to 3')
REC_F	AGTTCTCCAAGACAGGATCTTCTCATAAACGAGTTACCGAT CTTCCTCTGGGAGGTGGAGGTGGAGCT
REC_R	AGCGAACAGATTTGAAGATGCTTGACCTTAAAGATTGATC TACATCATCAGGCCCCAGCGGCCGCAGCAGCACC
3xYFP_SEQ F	AGCTATGTCTAAGGGTGAAGAACTC
3xYFP_SEQ R	CACCCTCGCCTTCTCCACTCACAG

b. Immunochemical techniques

For western blot analysis, frozen shoot and root tissues (0.1 g) were ground in liquid nitrogen into a fine powder and resuspended in 250 µl of 2X Laemmli SDS sample buffer (Laemmli, 1970). Proteins were separated by SDS-PAGE on 10% (w/v) polyacrylamide gels and proteins were transferred to Immobilon-P polyvinylidene fluoride membrane (PVDF; Millipore Corporation, Bedford, MA, U.S.A). Blotted membranes were blocked overnight in 10% (w/v) nonfat dry milk (NFDM) and 2% (v/v) goat serum in phosphate buffered saline (PBS) which is 10 mM NaPO₄, pH 7.2, 0.15 M NaCl at 4° C. Monoclonal anti-GFP antibody (1:2000; kind gift from Dr. Rose Goodchild, The University of Tennessee, Knoxville) and peroxidase-labeled horse anti-mouse IgG

(H+L) secondary antibody (1:2000; Vector Laboratories, Inc., Burlingame, CA, U.S.A) incubations were performed for 1 hr at 37° C in 2% (w/v) NFDM and 0.5% (v/v) goat serum in PBS pH 7.2. Chemiluminescent detection was done by incubation of membrane with 10 mL of 1.25 mM luminol, 0.2 mM *p*-coumaric acid, and 0.009% (v/v) hydrogen peroxide in 0.1 M Tris-HCl pH 8.5.

c. Genotyping of *NIP2;1promoter::NIP2;1:YFP* seedlings

For PCR genotyping, genomic DNA was extracted from 12-day-old recombineering seedlings that showed 100% antibiotic resistance. ~200 mg of leaf tissue in a 1.5 ml centrifuge tube was ground with a pestle in 500 µL extraction buffer consisting of 200 mM Tris-Cl (pH 7.0), 250 mM NaCl, 25 mM EDTA and 0.5% SDS, and was then vortexed and centrifuged at 13,000 rpm. Supernatant was added to a new tube and mixed with equal volume isopropanol, then again centrifuged. The pellet was washed with 75% (v/v) ethanol. After drying the sample, 100 µL deionized water was added, vortexed, and centrifuged as described above. For PCR amplification, 1 µl of the genomic DNA was used as template in combination with 100 nM 3X YFP F & R primers in a final volume of 25 µL with 1X GoTaq Green Master Mix (Promega). PCR reactions were performed using the following parameters: 94° C for 2 minutes; followed by 30 cycles of 94° C for 30 seconds, 53° C for 30 seconds, 72° C for 1 minute; with a final elongation cycle of 72° C for 5 minutes. 20 µl of the PCR product was loaded on a 1.2%

(w/v) agarose gel in Tris-acetate buffer and electrophoretic separation was performed under a constant voltage of 100 V for 30 minutes.

2.3 Microscopy

12-day-old *NIP2;1promoter::NIP2;1:YFP* seedlings challenged with hypoxia stress, as described above, were transferred onto microscopic glass slides and placed under a coverslip with water. Epifluorescence images were captured with Axiovert 200M microscope (Zeiss) equipped with filters for YFP fluorescence (Chroma, filter set 52017) and a digital camera (Hamamatsu Orca-ER) controlled by the Openlab software (Improvision). Confocal imaging was performed with a Hamamatsu camera mounted on an Olympus IX83 microscope with a Visitech confocal system. YFP excitation was kept at 514 nm and emission scans were taken using a long pass filter (525LP). For FM4-64FX dye (Molecular Probes 34653) plasma membrane staining, hypoxia challenged seedlings were incubated with 5 $\mu\text{g ml}^{-1}$ of dye in water for 5 minutes at room temperature in a 50 ml falcon tube. Seedlings were washed once with water prior to use for imaging analysis.

2.4 Metabolomics

Note: all work is done in a 4 °C cold room unless otherwise specified, and this portion of the work was performed with the assistance of the Mass Spectrometry Facility in the Department of Chemistry at the University of Tennessee, Knoxville.

a. Sample preparation

12 day-old WT and *NIP2;1promoter::NIP2;1:YFP* seedlings were subjected to hypoxia stress as described above. Shoot and root tissues were harvested from these seedlings and were immediately frozen in liquid nitrogen, and then stored at -80 °C until further use. For metabolite extraction, samples were grinded using a pestle and mortar with liquid nitrogen and powder was placed in a 1.5ml centrifuge tube. To each tube (~100mg of tissue powder) was added 1.3 mL of extraction solvent (40:40:20 HPLC grade methanol, acetonitrile, water with 0.1% formic acid) prechilled to 4 °C. Samples were vortexed to suspend particles and the extraction was allowed to proceed for 20 min at -20 °C. The samples were centrifuged for 5 min (16.1 rcf) at 4 °C. The supernatant was transferred to new 1.5 mL centrifuge tubes and the samples were resuspended with 100 µL of extraction solvent. Extraction was allowed to proceed for 20 min at -20 °C. The supernatant was transferred to the new centrifuge tubes and another 100 µL of extraction solvent was added to the samples repeating the previous extraction once more. The centrifuge tubes containing all of the collected supernatant liquid were centrifuged for 5 min (16.1 rcf) at 4 °C to remove any remaining particles and 1.2 mL were transferred to 1 dram vials. Vials containing 1.2 mL of the collected supernatant were dried under a stream of N₂ until all the extraction solvent had been evaporated. Solid residue was resuspended in 300 µL of sterile water and transferred to 300 µL autosampler vials. Samples were immediately placed in autosampler trays for mass spectrometric analysis.

b. UPLC-HRMS metabolomics analysis

Samples placed in an autosampler tray were kept at 4 °C. A 10 µL aliquot was injected through a Synergi 2.5 micron reverse phase Hydro-RP 100, 100 x 2.00 mm LC column (Phenomenex, Torrance, CA) kept at 25 °C. The eluent was introduced into the MS via an electrospray ionization source conjoined to an Exactive™ Plus Orbitrap Mass Spectrometer (Thermo Scientific, Waltham, MA) through a 0.1 mm internal diameter fused silica capillary tube. The mass spectrometer was run in full scan mode with negative ionization mode with a window from 85 – 1000 m/z. with a method adapted from (Lu et al., 2010). The samples were run with a spray voltage was 3 kV. The nitrogen sheath gas was set to a flow rate of 10 psi with a capillary temperature of 320 °C. AGC (acquisition gain control) target was set to 3e6. The samples were analyzed with a resolution of 140,000 and a scan window of 85 to 800 m/z for from 0 to 9 minutes and 110 to 1000 m/z from 9 to 25 minutes. Solvent A consisted of 97:3 water:methanol, 10 mM tributylamine, and 15 mM acetic acid. Solvent B was methanol. The gradient from 0 to 5 minutes is 0% B, from 5 to 13 minutes is 20% B, from 13 to 15.5 minutes is 55% B, from 15.5 to 19 minutes is 95% B, and from 19 to 25 minutes is 0% B with a flow rate of 200 µL/min.

Files generated by Xcalibur (RAW) were converted to the open-source mzML format (Martens et al., 2011) via the open-source msconvert software as part of the ProteoWizard package (Chambers et al., 2012). Maven (mzroll) software, Princeton University (Michelle F. Clasquin, Melamud, & Rabinowitz, 2012; Melamud, Vastag, &

Rabinowitz, 2010) was used to automatically correct the total ion chromatograms based on the retention times for each sample. (M. F. Clasquin, Melamud, & Rabinowitz, 2002; Melamud et al., 2010). Metabolites were manually identified and integrated using known masses (± 5 ppm mass tolerance) and retention times ($\Delta \leq 1.5$ min). Unknown peaks were automatically selected via Maven's automated peak detection algorithms.

Fold changes were calculated using Excel 2010 (Microsoft Corporation, Redmond, WA). The data were transformed and clustered using Cluster software (Eisen, Spellman, Brown, & Botstein, 1998). Heatmaps were then generated using Java Treeview5 software (Saldanha, 2004). PCA (principal component analysis) were performed and figures were generated using the statistical package R version 3.1.1 (Team, 2013) along with the ggplot2 (Wickham, 2009) and ggbiplot (Vu, 2011) packages. PLS-DA (Partial Least Squares Discriminant Analysis) plots were also generated via R along with the mixOmics (Dejean S & F, 2014) package using metabolite areas as the predictors and mouse type as the discrete outcomes with a tolerance of 1×10^{-6} and a max iteration of 500.

III. RESULTS

3.1 NIP2;1 levels in shoot and root tissue during hypoxia

Western blot analysis was performed to verify the hypoxia trigger induction of NIP2;1 protein in recombinering plants. Plant shoot and root tissue of 12-day-old seedlings were collected at 2-hour intervals between 0 and 6 hours of flooding treatment. Plant shoot tissue showed no protein expression, while root tissue from 4 to 6 hours showed increased levels of NIP2;1 protein in comparison to 0 and 2 hours (Fig. 6), consistent with hypoxia induced, root-specific expression as reported by Choi and Roberts (2007).

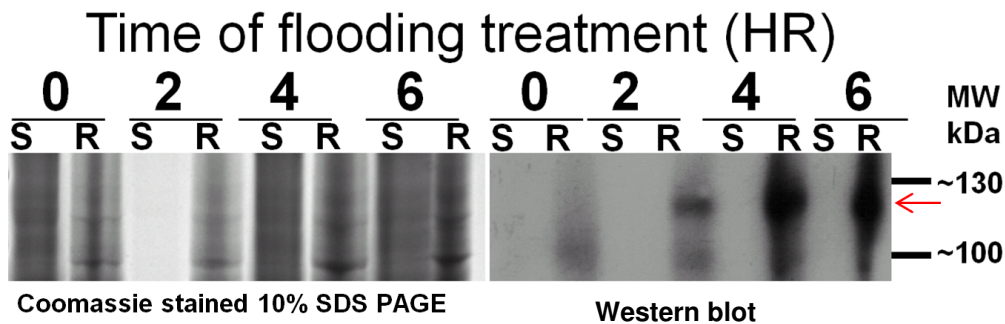


Figure 6. AtNIP2;1 protein level in shoot and root tissue of hypoxia challenged 12-day-old *Arabidopsis* seedlings. Protein separation is based on size by gel electrophoresis using Coomassie stained 10% SDS gel and identified by Western blot. AtNIP2;1 protein expression from 0 to 6 hours (HR) of flooding in shoot (S) and root (R) tissue was observed. Root tissue after 4-6 hours showed the highest level of AtNIP2;1 protein expression. An arrow indicates protein of interest (AtNIP2;1, accounting for triple YFP tag) with a molecular weight (MW) of ~112 kDa.

3.2 NIP2;1 subcellular localization

As noted above, hypoxia induces the expression of *AtNIP2;1* and cellular analysis of flooding stressed *AtNIP2;1 promoter::GUS* transgenic seedlings showed high expression in the root stele containing the vascular cylinder, as well as in cortical cells and lateral roots (Choi & Roberts, 2007). It has been suggested that *AtNIP2;1* is an anaerobic polypeptide demonstrating expression selective to root tissue (Choi, 2009). The present study has investigated the localization of NIP2;1 using fluorescent protein fusions of *AtNIP2;1* protein (*NIP2;1promoter::NIP2;1:YFP*). Determining cellular localization in hypoxic *Arabidopsis* roots allows us to better understand its biological function.

Recombineering transgenic *Arabidopsis* plants with terminal YFP fusion constructs were used to determine subcellular localization through fluorescence microscopy. Based on our western blot analysis (Fig. 6), it appears that NIP2;1 levels are substantially higher at 6 hr. Therefore, for subcellular localization studies we chose to examine NIP2;1:YFP seedlings after 6 hr of flooding treatment using fluorescence microscopy. Expression of *AtNIP2;1* results in localization that appears to be distinct from the cytosol and nucleus (Fig. 7). Furthermore, we observed NIP2;1 proteins specifically localizing to the root stele, presumably in the phloem vascular tissue (Fig. 7). In some micrographs, polarized localization to the ends of phloem cells can be observed (Fig. 8). DIC images show the architecture of cells, and higher magnification in confocal microscopy supports our fluorescence study and shows that NIP2;1 is exclusive to the root stele.

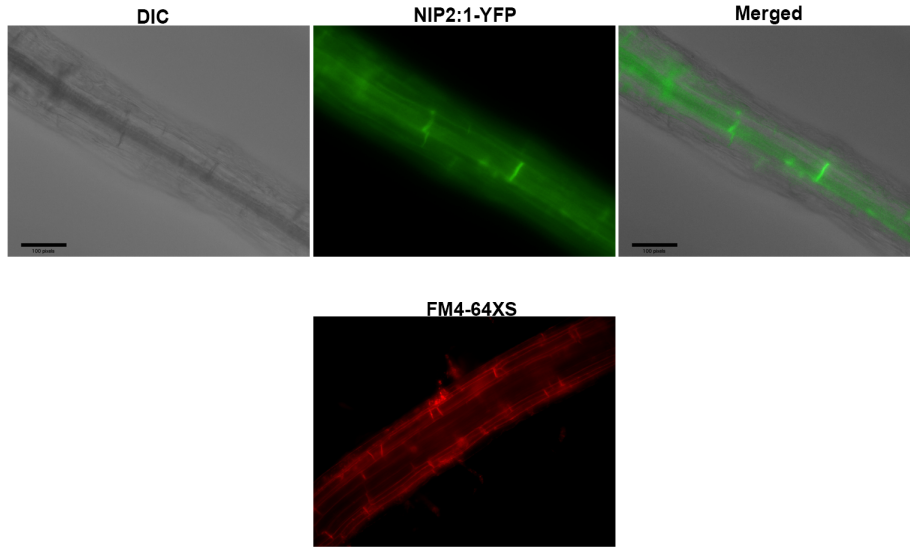


Figure 7. Fluorescence imaging of recombineering plants dyed with FM4-64X.

NIP2;1 promoter::NIP2;1:YFP recombineering seedlings were stained with FM4-64X, a plasma membrane specific dye, and imaged

by fluorescent microscopy. The scale bar represents 100 pixels. The DIC (optical differential inference contrast) image shows root architecture. Plasma membrane cells were stained to determine that localization is observed in cell membranes in the root stele.

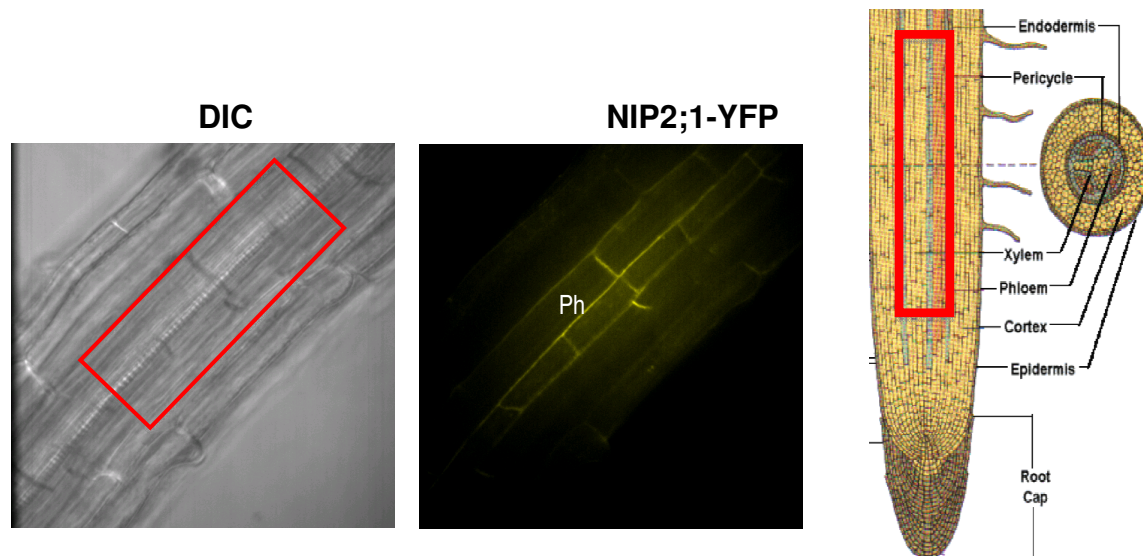


Figure 8. Fluorescence imaging of recombineering plants. *Arabidopsis* seedlings with yellow fluorescent protein tag associated with AtNIP2;1 (*NIP2;1 promoter::NIP2;1:YFP*) were imaged by fluorescent microscopy. AtNIP2;1 protein localization is observed within the root stele that contains the vascular cylinder (red box). The DIC (optical differential inference contrast) image shows root architecture. Longitudinal root architecture is shown for comparison ("World Book Encyclopedia," 1979) with a red box indicating the position of the stele. "Ph" indicates the location of the phloem.

A plasma membrane specific dye, FM4-64FX (Molecular Probes 34653), was additionally used to stain *Arabidopsis* root tissue. FM4-64X was used because it enables the cell membrane to be dyed and emphasized to determine protein localization in the plasma membrane. This indicates that expression of NIP2;1 results in localization on the plasma membrane in the root stele (Fig. 8). This also supports prior research that found NIP2;1 to localize around the cell periphery of *Arabidopsis* mesophyll protoplasts, indicating that NIP2;1 is a cell membrane protein (Choi & Roberts, 2007).

3.3 Metabolic profile of WT and *AtNIP2;1* T-DNA knockout

The finding that NIP2;1 is associated with prospective phloem vascular cells under hypoxia suggests that it participates in the transport of lactic acid through this tissue, perhaps as part of adaptive response to prevent lactic acid toxicity. To test this hypothesis, the organic acid content of tissue from wild type and *nip2;1* T-DNA knockout plants was evaluated by metabolomic analysis. Metabolomic studies measure the levels of a multitude of metabolites at a given moment, providing a snapshot of the metabolic state of the entire system. Heat maps are applied to easily compare this large quantity of data, representing relative abundance with differing color intensity (Ivanisevic et al., 2014). This study examined the metabolic profile of *Arabidopsis* wild type and *AtNIP2;1* gene knockout seedlings at different time intervals of flooding stress to investigate the effects of AtNIP2;1 protein on various metabolites, with a strong emphasis on lactic acid. Other metabolites, such as alanine, were also considered due to the ability of

lactate dehydrogenase (LDH) to catalyze the reverse reaction of lactate to pyruvate, which can then be converted to alanine by the action of amino transferase enzymes.

Metabolite levels in roots and shoots were compared at 0 and 6 hours of flooding treatment, with bright red on the metabolomic heat map indicating the highest comparative levels and blue indicating the lowest. Since *NIP2;1* is a putative lactic acid channel, we chose to focus on the comparative lactic acid levels in wild type and knockout plants (Fig. 9). We observed that lactate levels are significantly higher in the WT roots than in the WT shoots in normoxic plants (0 hr) and hypoxic plants (6 hr), although a higher apparent ratio of lactic acid in shoots:roots is observed at 6 hr (Fig. 9A).

In comparison, *AtNIP2;1* knockout seedlings show a lower shoot:root ratio of lactic acid compared to wild type, and there is no apparent difference between normoxic and hypoxic plants (Fig. 9B). This suggests that the loss of *AtNIP2;1* results in a difference in the lactic acid partitioning between these two tissues.

Since *AtNIP2;1* is a selective transporter of lactic acid as a substrate, we propose that a knockout of the *AtNIP2;1* gene results in a reduced efflux of lactic acid from fermenting cells, and that lactic acid remains higher in these cells.

For both WT and *AtNIP2;1* knockout seedlings, alanine levels decreased in the roots from 0 to 6 hr and increased in the shoots from 0 to 6 hr (Fig. 9A,B).

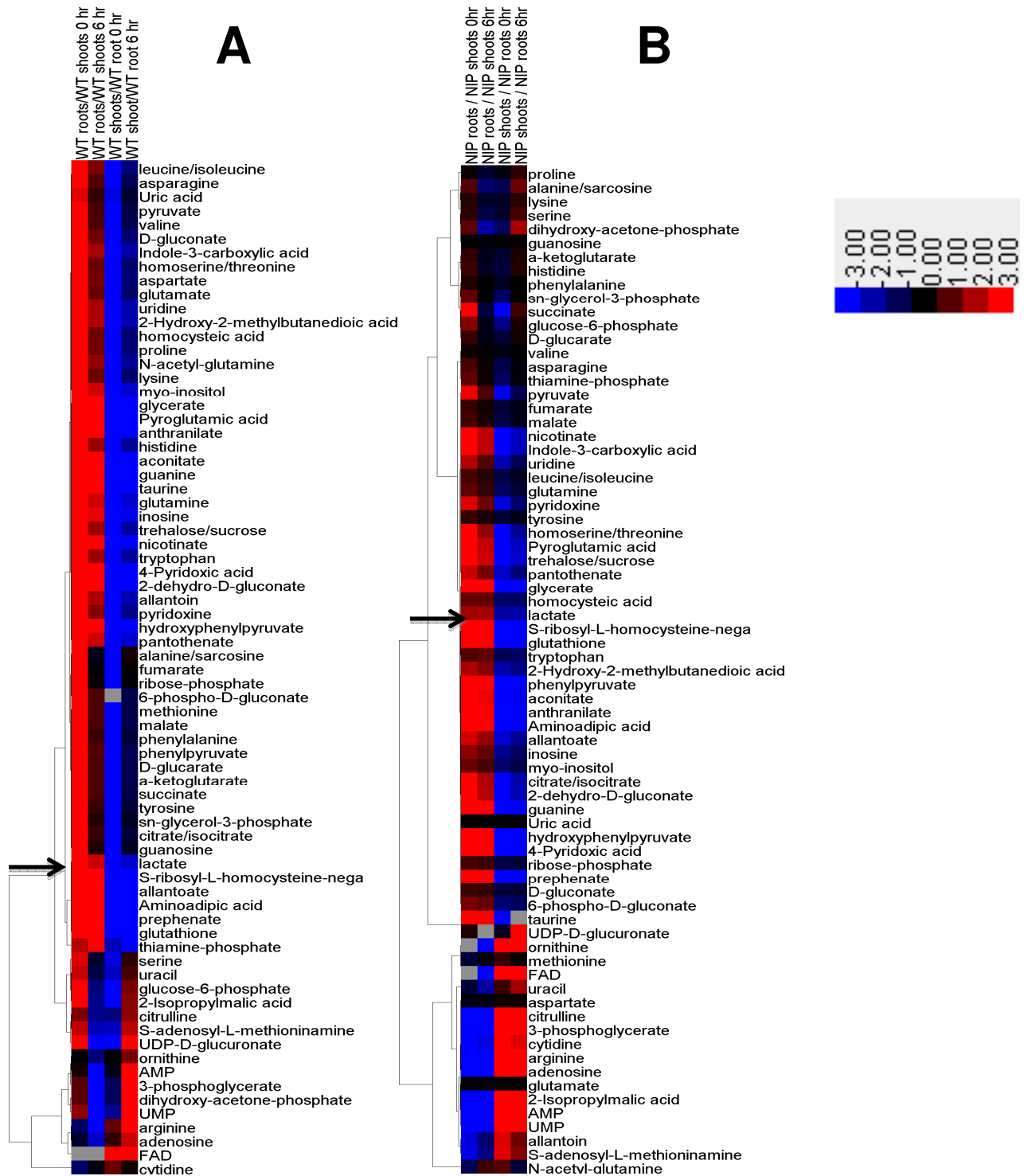


Figure 8. Heat map of metabolomics of *Arabidopsis* WT (A) and *AtNIP2;1* gene knockouts (B).

Shoot and root tissue is collected and analyzed at 0-6 hr intervals. A heat map scale is provided with a range of -3 → 0 → 3, with bright red indicating the highest comparative levels and blue indicating the lowest. Lactate is indicated with arrows on the heat map for *Arabidopsis* WT and *AtNIP2;1* knockouts.

IV. DISCUSSION AND CONCLUSION

The present study has investigated the localization of *AtNIP2;1* using fluorescent versions of NIP2;1 protein to analyze cellular localization in hypoxic *Arabidopsis* roots. We have also investigated relevant metabolite profiling of NIP2;1 knockout and wild type plants, with a focus on lactic acid. Evidence from our studies supports the hypothesis that NIP2;1 acts as a lactic acid efflux channel that localizes in the root stele. We additionally propose that NIP2;1 specifically localizes to the phloem vascular cells within the root stele, and propose a model through which NIP2;1 participates in transport of lactic acid from plant roots to shoots.

It has been previously observed that *AtNIP2;1*, as well as most NIPs, have a much lower level of expression in normoxic *Arabidopsis* seedlings compared to other plant NIPs. However, *AtNIP2;1* is known to be responsive to signals of environmental stress such as flooding, and acute induction of its expression has particularly been seen in response to anaerobic stress (Choi & Roberts, 2007). A rapid 70-fold increase in *AtNIP2;1* transcript level has been observed by Q-PCR after 1 hour of flooding 2-week-old seedlings (Choi & Roberts, 2007). Expression then decreased after 6 hours, but still maintained a 10- to 20-fold level above control transcript levels. GUS staining of flooding stressed *AtNIP2;1 promoter::GUS* transgenic seedlings, which respond to stress by producing beta-glucuronidase (GUS) and turning a blue color in affected tissues, also exhibited a rapid increase in expression at 1 hour (Choi & Roberts, 2007). High expression was observed in the vascular cylinder (i.e., the root stele), as well as in

cortical cells and lateral roots. It has been suggested that *AtNIP2;1* is an anaerobic polypeptide demonstrating expression selective to root tissue (Choi & Roberts, 2007).

We further suggest that *AtNIP2;1* encodes for a protein transporter exhibiting unique protonated lactic acid preference and activity. This could be explained by the need for an adaptation mechanism allowing for the cytosolic efflux of lactic acid, a toxic fermentation end product. It can furthermore be suggested that, in order to mediate lactic acid efflux to prevent cytosolic acidosis, NIP2;1 localizes to the root stele to traffic lactic acid out of root tissue. Specifically, one hypothetical role of NIP2;1 is to mediate lactic acid efflux by localizing to the phloem of the root stele to perform this function (Fig. 10). Transporting lactic acid out of plant roots and into shoot tissue could minimize damage to root cells, with the phloem serving as a global response link between roots and shoots to best preserve the plant during times of stress.

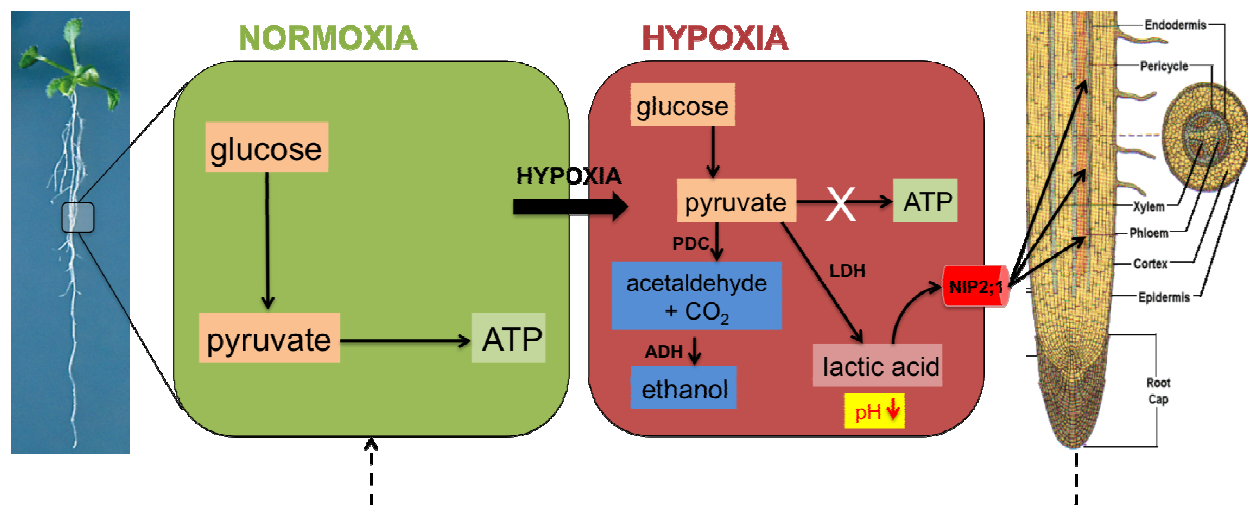


Figure 9. Schematics of NIP2;1 function under hypoxia stress. Energy catabolism is interrupted as a result of hypoxia and flooding stress. NADH must be recycled in order to maintain glycolysis, but this leads to an accumulation of H^+ (cytosolic acidosis). NIP2;1 localizes to the root stele to serve as a lactic acid efflux channel, in which we propose localization is specific to the phloem in order to traffic lactic acid to plant shoots. Additionally, plants switch to ethanolic fermentation to prevent a further decline in pH. These response mechanisms prevent subsequent root tissue damage. *Arabidopsis* root image is from (Mashiguchi et al., 2011); longitudinal root architecture image is from ("World Book Encyclopedia," 1979).

4.1 NIP2;1 is a lactic acid transporter induced by anaerobic stress

Metabolomics experiments demonstrate that lactic acid levels are high in wild type *Arabidopsis* root tissue shortly after being subjected to hypoxic conditions. A comparative increase is then observed in shoot tissue after a 6-hour period. It is possible that lactic acid is undergoing efflux from the roots into the shoots as a global, coordinated response to prevent cytosolic acidosis. This is also in accordance with the Davies-Roberts hypothesis, in which plants switch from lactic acid fermentation to ethanolic fermentation (Davies, Grego, & Kenworthy, 1974; Roberts, Callis, Wemmer,

Walbot, & Jardetzky, 1984). Lactic acid fermentation leads to an increase in cytosolic proton levels, leading to excessive acidity. To prevent tissue damage, the plant converts to ethanolic fermentation, which does not produce protons. However, there is still the need to transport either lactic acid or lactate and H⁺ out of the cell. As MIPs transport uncharged metabolites (Agre et al., 2002), this further supports the evidence that NIP2;1 transports the uncharged protonated form of this molecule, as well as serves for this stress response mechanism in *Arabidopsis*.

The metabolite profiling conducted is limited to a certain time point, and metabolites in *Arabidopsis* are always undergoing various reactions, particularly during a period of stress. Lactate dehydrogenase can instead catalyze the reversible oxidation of lactate to pyruvate, which can subsequently be converted to alanine. As discussed by Mustroph, Barding, Kaiser, Larive, and Bailey-Serres (2014), alanine accumulation could play a role in decreasing pyruvate levels to circumvent inhibition of glycolysis, to store carbon and nitrogen for accessible harvest, or to be recycled in the shoot tissue. The metabolite profile is helpful for this reason, but further research should be done.

We additionally observed that *AtNIP2;1* knockouts, although experiencing a slight increase in lactic acid levels, did not undergo relative metabolic change. This can be explained due to the lack of the NIP2;1 protein to efflux lactic acid. Instead, the lactic acid in the knockout plants is not transported and remains within the fermenting cells where it is produced. However, these plants could still develop other potential means to compensate for the loss of the *AtNIP2;1* stress response gene. *AtNIP2;1* knockout

plants may be more tolerant to low oxygen stress than are their wild type counterparts due to the creation of a “pre-adaptation” state (Choi, 2009).

4.2 NIP2;1 is localized to the phloem of the root stele

Plants ultimately adapt to low oxygen stress conditions in three ways, enacting both short-term and long-term methods. These include an increase in glycolytic flux to provide ATP (the Pasteur Effect), an increase in fermentation metabolism to continue regenerating NAD^+ needed for glycolysis, and eventual morphological changes in development that will aid in increasing absorbed O_2 levels (Drew, 1997). As previously mentioned, though an increase in fermentation metabolism is necessary to sustain life, it eventually causes harm due to its toxic byproducts. Though it is understood that NIP2;1 is a transporter of lactic acid, it is imperative to investigate where this lactic acid is transported to and why.

Experiments employing confocal microscopy with recombineering plant roots demonstrates that NIP2;1 localizes to the plasma membrane of cells in the root stele. More specifically, it can be suggested that NIP2;1 localizes to the phloem of the root stele. This is further supported by the metabolomics results suggesting that lactic acid is being transported, and could be mobilized from plant roots into shoots for further metabolism. Based on localization analyses, this transportation is proposed to occur through the phloem, which is also responsible for transporting water and nutrients in a source to sink manner. Therefore, it can be argued that the phloem has additional

purposes that contribute to transport of potentially harmful metabolites as part of stress response adaptation mechanisms.

Therefore, not only does NIP2;1 act as an efflux channel for lactic channel, but its localization to the phloem could serve to transport lactic acid from root tissue to plant shoots in order to dispose or recycle this toxic compound and avoid cytosolic acidosis. Root tissue, despite its established anaerobic response mechanisms, is likely to be more vulnerable during hypoxia and flooding. As this study indicates, it is probable that *Arabidopsis* shoots can aid in partially offsetting this stress. The link between root and shoot tissue would serve as a global response mechanism to stress, but more research should be done in order to support these findings. Additionally, further studies should be conducted to better understand the interactions of metabolites on a global level and what their ultimate fates are during the flooding and hypoxia stress response.

V. REFERENCES

- Agre, P., King, L. S., Yasui, M., Guggino, W. B., Ottersen, O. P., Fujiyoshi, Y., . . . Nielsen, S. (2002). Aquaporin water channels--from atomic structure to clinical medicine. *J Physiol*, *542*(Pt 1), 3-16.
- Bailey-Serres, J., & Colmer, T. D. (2014). Plant tolerance of flooding stress –recent advances. *Plant Cell Environ*, *37*(10), 2211-2215. doi: 10.1111/pce.12420
- Buchanan, B. B., Gruissem, W., & Jones, R. L. (2000). *Biochemistry & molecular biology of plants*. Rockville, Md.: American Society of Plant Physiologists.
- Chambers, M. C., Maclean, B., Burke, R., Amodei, D., Ruderman, D. L., Neumann, S., . . . Mallick, P. (2012). A cross-platform toolkit for mass spectrometry and proteomics. *Nature Biotechnology*, *30*(10), 918-920. doi: 10.1038/nbt.2377
- Chaumont, F., Moshelion, M., & Daniels, M. J. (2005). Regulation of plant aquaporin activity. *Biol Cell*, *97*(10), 749-764. doi: 10.1042/BC20040133
- Choi, W. G. (2009). *Nodulin 26-like Intrinsic Protein NIP2;1 and NIP7;1: Characterization of transport function and roles in developmental and stress responses in Arabidopsis*. (Doctor of Philosophy), The University of Tennessee, Knoxville, TN.
- Choi, W. G., & Roberts, D. M. (2007). Arabidopsis NIP2;1, a major intrinsic protein transporter of lactic acid induced by anoxic stress. *J Biol Chem*, *282*(33), 24209-24218. doi: 10.1074/jbc.M700982200

- Clasquin, M. F., Melamud, E., & Rabinowitz, J. D. (2002). *LC-MS Data Processing with MAVEN: A Metabolomic Analysis and Visualization Engine* (Current Protocols in Bioinformatics ed.): John Wiley & Sons, Inc.
- Clasquin, M. F., Melamud, E., & Rabinowitz, J. D. (2012). LC-MS data processing with MAVEN: a metabolomic analysis and visualization engine. *Current protocols in bioinformatics / editorial board, Andreas D. Baxevanis ... [et al.]*, Chapter 14, Unit14.11. doi: 10.1002/0471250953.bi1411s37
- Davies, D. D., Grego, S., & Kenworthy, P. (1974). The control of the production of lactate and ethanol by higher plants. *Planta*, 118(4), 297-310. doi: 10.1007/BF00385580
- Dejean S, G. I., Le Cao K, Monget P, Coquery J, Yao F, Liquet B., & F, R. (2014). mixOmics: Omics Data Integration Project. Retrieved from <http://CRAN.R-project.org/package=mixOmics>
- Drew, M. C. (1997). OXYGEN DEFICIENCY AND ROOT METABOLISM: Injury and Acclimation Under Hypoxia and Anoxia. *Annu Rev Plant Physiol Plant Mol Biol*, 48, 223-250. doi: 10.1146/annurev.arplant.48.1.223
- Eisen, M. B., Spellman, P. T., Brown, P. O., & Botstein, D. (1998). Cluster analysis and display of genome-wide expression patterns. *Proceedings of the National Academy of Sciences of the United States of America*, 95(25), 14863-14868. doi: 10.1073/pnas.95.25.14863
- Fu, D., Libson, A., Miercke, L. J., Weitzman, C., Nollert, P., Krucinski, J., & Stroud, R. M. (2000). Structure of a glycerol-conducting channel and the basis for its selectivity. *Science*, 290(5491), 481-486.

- Gomes, D., Agasse, A., Thiebaud, P., Delrot, S., Geros, H., & Chaumont, F. (2009). Aquaporins are multifunctional water and solute transporters highly divergent in living organisms. *Biochim Biophys Acta*, 1788(6), 1213-1228. doi: 10.1016/j.bbamem.2009.03.009
- Gorin, M. B., Yancey, S. B., Cline, J., Revel, J. P., & Horwitz, J. (1984). The major intrinsic protein (MIP) of the bovine lens fiber membrane: characterization and structure based on cDNA cloning. *Cell*, 39(1), 49-59.
- Ivanisevic, J., Benton, H. P., Rinehart, D., Epstein, A., Kurczy, M. E., Boska, M. D., . . . Siuzdak, G. (2014). An interactive cluster heat map to visualize and explore multidimensional metabolomic data. *Metabolomics*.
- Jackson, M. B., & Colmer, T. D. (2005). Response and adaptation by plants to flooding stress. *Ann Bot*, 96(4), 501-505.
- Johanson, U., Karlsson, M., Johansson, I., Gustavsson, S., Sjoval, S., Frayse, L., . . . Kjellbom, P. (2001). The complete set of genes encoding major intrinsic proteins in *Arabidopsis* provides a framework for a new nomenclature for major intrinsic proteins in plants. *Plant Physiol*, 126(4), 1358-1369.
- Johansson, I., Karlsson, M., Johanson, U., Larsson, C., & Kjellbom, P. (2000). The role of aquaporins in cellular and whole plant water balance. *Biochim Biophys Acta*, 1465(1-2), 324-342.
- Jung, J. S., Preston, G. M., Smith, B. L., Guggino, W. B., & Agre, P. (1994). Molecular structure of the water channel through aquaporin CHIP. The hourglass model. *J Biol Chem*, 269(20), 14648-14654.

- Laemmli, U. K. (1970). Cleavage of structural proteins during the assembly of the head of bacteriophage T4. *Nature*, *227*(5259), 680-685.
- Lu, W. Y., Clasquin, M. F., Melamud, E., Amador-Noguez, D., Caudy, A. A., & Rabinowitz, J. D. (2010). Metabolomic Analysis via Reversed-Phase Ion-Pairing Liquid Chromatography Coupled to a Stand Alone Orbitrap Mass Spectrometer. *Analytical Chemistry*, *82*(8), 3212-3221. doi: 10.1021/ac902837x
- Ludewig, U., & Dynowski, M. (2009). Plant aquaporin selectivity: where transport assays, computer simulations and physiology meet. *Cell Mol Life Sci*, *66*(19), 3161-3175. doi: 10.1007/s00018-009-0075-6
- Martens, L., Chambers, M., Sturm, M., Kessner, D., Levander, F., Shofstahl, J., . . . Deutsch, E. W. (2011). mzML-a Community Standard for Mass Spectrometry Data. *Molecular & Cellular Proteomics*, *10*(1). doi: 10.1074/mcp.R110.000133
- Mashiguchi, K., Tanaka, K., Sakai, T., Sugawara, S., Kawaide, H., Natsume, M., . . . Kasahara, H. (2011). The main auxin biosynthesis pathway in Arabidopsis. *Proc Natl Acad Sci U S A*, *108*(45), 18512-18517. doi: 10.1073/pnas.1108434108
- Maurel, C., Verdoucq, L., Luu, D. T., & Santoni, V. (2008). Plant aquaporins: membrane channels with multiple integrated functions. *Annu Rev Plant Biol*, *59*, 595-624. doi: 10.1146/annurev.arplant.59.032607.092734
- Melamud, E., Vastag, L., & Rabinowitz, J. D. (2010). Metabolomic Analysis and Visualization Engine for LC-MS Data. *Analytical Chemistry*, *82*(23), 9818-9826. doi: 10.1021/ac1021166
- Mustroph, A., Barding, G. A., Jr., Kaiser, K. A., Larive, C. K., & Bailey-Serres, J. (2014). Characterization of distinct root and shoot responses to low-oxygen stress in

- Arabidopsis with a focus on primary C- and N-metabolism. *Plant Cell Environ*, 37(10), 2366-2380. doi: 10.1111/pce.12282
- Mustroph, A., Zanetti, M. E., Jang, C. J., Holtan, H. E., Repetti, P. P., Galbraith, D. W., . . . Bailey-Serres, J. (2009). Profiling transcriptomes of discrete cell populations resolves altered cellular priorities during hypoxia in Arabidopsis. *Proc Natl Acad Sci U S A*, 106(44), 18843-18848. doi: 10.1073/pnas.0906131106
- Preston, G. M., Carroll, T. P., Guggino, W. B., & Agre, P. (1992). Appearance of water channels in Xenopus oocytes expressing red cell CHIP28 protein. *Science*, 256(5055), 385-387.
- Roberts, J. K., Callis, J., Wemmer, D., Walbot, V., & Jardetzky, O. (1984). Mechanisms of cytoplasmic pH regulation in hypoxic maize root tips and its role in survival under hypoxia. *Proc Natl Acad Sci U S A*, 81(11), 3379-3383.
- Saldanha, A. J. (2004). Java Treeview-extensible visualization of microarray data. *Bioinformatics*, 20(17), 3246-3248. doi: 10.1093/bioinformatics/bth349
- Smith, B. L., & Agre, P. (1991). Erythrocyte Mr 28,000 transmembrane protein exists as a multisubunit oligomer similar to channel proteins. *J Biol Chem*, 266(10), 6407-6415.
- Sorani, M. D., Manley, G. T., & Giacomini, K. M. (2008). Genetic variation in human aquaporins and effects on phenotypes of water homeostasis. *Hum Mutat*, 29(9), 1108-1117. doi: 10.1002/humu.20762
- Sui, H., Han, B. G., Lee, J. K., Walian, P., & Jap, B. K. (2001). Structural basis of water-specific transport through the AQP1 water channel. *Nature*, 414(6866), 872-878. doi: 10.1038/414872a

- Tanaka, M., Wallace, I. S., Takano, J., Roberts, D. M., & Fujiwara, T. (2008). NIP6;1 is a boric acid channel for preferential transport of boron to growing shoot tissues in *Arabidopsis*. *Plant Cell*, *20*(10), 2860-2875. doi: 10.1105/tpc.108.058628
- Team, R. C. (2013). R: A language and environment for statistical computing. R Foundation for Statistical Computing, Vienna, Austria.
- Vartapetian, B. B., & Jackson, M. B. (1997). Plant Adaptations to Anaerobic Stress. *Ann Bot*, *79*, 3-20.
- Voesenek, L. A., & Bailey-Serres, J. (2015). Flood adaptive traits and processes: an overview. *New Phytol*, *206*(1), 57-73. doi: 10.1111/nph.13209
- Vu, V. Q. (2011). ggbiplot: A ggplot2 based biplot. Retrieved from <http://github.com/vqv/ggbiplot>
- Wallace, I. S., Choi, W. G., & Roberts, D. M. (2006). The structure, function and regulation of the nodulin 26-like intrinsic protein family of plant aquaglyceroporins. *Biochim Biophys Acta*, *1758*(8), 1165-1175. doi: 10.1016/j.bbamem.2006.03.024
- Wallace, I. S., & Roberts, D. M. (2004). Homology modeling of representative subfamilies of Arabidopsis major intrinsic proteins. Classification based on the aromatic/arginine selectivity filter. *Plant Physiol*, *135*(2), 1059-1068. doi: 10.1104/pp.103.033415
- Wickham, H. (2009). *ggplot2: elegant graphics for data analysis*: Springer New York.
- World Book Encyclopedia. (1979). Chicago: World Book-Childcraft International, Inc.

Zhou, R., Benavente, L. M., Stepanova, A. N., & Alonso, J. M. (2011). A recombineering-based gene tagging system for Arabidopsis. *Plant J*, 66(4), 712-723. doi: 10.1111/j.1365-313X.2011.04524.x